2013

Interference Cancellation in Wideband Receivers using Compressed Sensing

Tejaswi C. Peyyeti
University of Massachusetts Amherst

INTERFERENCE CANCELLATION IN WIDEBAND RECEIVERS USING COMPRESSED SENSING

A Thesis Presented

by

TEJASWI CHAITANYA PEYYETI

Submitted to the Graduate School of the
University of Massachusetts Amherst in partial fulfillment
of the requirements for the degree of

MASTER OF SCIENCE IN ELECTRICAL AND COMPUTER ENGINEERING

February 2013

Electrical and Computer Engineering

INTERFERENCE CANCELLATION IN WIDEBAND RECEIVERS USING COMPRESSED SENSING

A Thesis Presented

by

TEJASWI CHAITANYA PEYYETI

Approved as to style and content by:

Dennis L. Goeckel, Chair

Robert W. Jackson, Member

Marco F. Duarte, Member

C. V. Hollot, Department Chair
Electrical and Computer Engineering

To my family and Sai Baba.

ACKNOWLEDGEMENT

I would like to thank all people who have encouraged, instilled confidence and supported me in my difficult phases. Specifically, my adviser Prof. Dennis L. Goeckel who has guided me at every stage of my thesis, my fellow labmate and Ph.D candidate Cagatay Capar and my best friends KC, Paul and Ashwin.

I would like to thank Prof. Jackson and Prof. Duarte who have agreed to be part of my thesis committee and have provided valuable advice.

ABSTRACT

INTERFERENCE CANCELLATION IN WIDEBAND RECEIVERS USING COMPRESSED SENSING

FEBRUARY 2013

TEJASWI CHAITANYA PEYYETI

M.S.E.C.E., UNIVERSITY OF MASSACHUSETTS AMHERST

Directed by: Professor Dennis L. Goeckel

Previous approach for narrowband interference cancellation based on compressed sensing (CS) in wideband receivers uses orthogonal projections to project away from the interference. This is not effective in the presence of nonlinear LNA (low noise amplifier) and finite bit ADCs (analog-to-digital converters) due to the fact that the nonidealities present will result in irresolvable intermodulation components and corrupt the signal reconstruction. Cancelling out the interferer before reaching the LNA thus becomes very important. A CS measurement matrix with randomly placed zeros in the frequency domain helps in this regard by removing the effect of interference when the signal measurements are performed before the LNA. Using this idea, under much idealized hardware assumptions impressive performance is obtained.

The use of binary sequences which makes the hardware implementation simplistic is investigated in this thesis. Searching sequences with many spectral nulls turns out to be nontrivial. A theoretical approach for estimating probability of nulls is provided to reduce significant computational effort in the search and is shown to be close to actual search iterations. The use of real binary sequences (generated using ideal switches) obtained through

the search does not do better compared to the orthogonal projection method in the presence of nonlinear LNA.

TABLE OF CONTENTS

LIST OF FIGURES

Figure **Page**

CHAPTER 1

INTRODUCTION

Narrowband interference in wideband wireless systems can result in the saturation of the RF front-end and a high bit error rate with a severe drop in the receiver sensitivity. These RF(radio frequency) impairments are largely caused by nonlinear blocks such as the LNA (low noise amplifier) in the front end [20]. Approaches to the mitigation of this problem have focused on the use of filters for removing the out-of-band signals or to cancel out the in-band interferer [9] under the assumption of knowledge of the interferer. These come with the price of additional nonlinearity and implementation complexity. In this context, this thesis is focused on the extraction of weak signals in strong interference in wideband systems through the use of approaches based on compressed sensing. The previous work in this area uses orthogonal projections at baseband to cancel out interference and filter the signal of interest [15]. But in reality, the nonlinearities in the front-end due to the LNA and the inaccurate quantization of finite resolution ADCs (analog-to-digital converters) affects the reconstruction severely and thus in practice these projection approaches often show no tangible interference cancellation. In this thesis, we propose a different interference cancellation method using the insertion of frequency domain nulls in the measurement matrix in a compressed sensing system.

1.1 Wideband interference problem

The system bandwidth of wireless communication devices in the future will be huge due to the need to accommodate advanced communication systems such as cognitive and software radios, surveillance applications, multi-function radios, environmental sensing

etc. In particular, radio receivers that are reconfigurable and highly-flexible are needed in order to meet these demands. For applications such as cognitive radio, a very wide bandwidth (of the order of GHz) needs to be monitored by the receivers. The presence of interfering signals cannot be neglected in such a wide band, as their presence heavily impacts the performance of receivers in resolving the weak signals of interest. Traditional receivers consist of downconversion blocks followed by digitization by ADCs (analog-to-digital converter) and the backend DSP (digital signal processor) where the signal processing matched to the application is done. The presence of high power interferers which are often due to an interfering transmitter being very near to the receivers raise the dynamic range requirements of the ADC in the front end. However, it is known that ADCs at very high bandwidths are complex and consume high power [19]. In this regard, newly emerged compressed sensing-based hardware architectures [11, 13, 14] have been built and implemented successfully where the sampling can be done at the *information rate* rather than the Nyquist rate by employing certain nonlinear reconstruction techniques. By assuming a linear model for the RF front-end processing, current techniques of interference mitigation based on compressed sensing [15, 16] have primarily concentrated on utilizing the DSP to project away from the interference. But this linearity assumption is not realistic as circuit designers cannot avoid having some nonlinearity in components such as LNAs.

Methods such as tunable filters or MEMs filters [9] that mitigate interference before reaching the LNA add noise and bring their own nonlinearity, so are not an attractive solution. To make the front-end linear, a high value of IIP3 (third order input referred intercept point) is required. LNA designs have been built to achieve good values of IIP3, but these involve complicated digitial signal processing [10]. Hence these solutions have not been commercially deployed yet, leaving the wideband interference problem open. Thus, the goal of this thesis is to develop algorithmic methods to combat the challenging problem of interference mitigation in the presence of nonlinearities in the receiver front-end of wideband wireless communication systems.

1.2 Compressed Sensing

As the data rates in a wide range of applications rise, there is a growing need to efficiently acquire, store and process such a high deluge of data. This requirement places a massive burden on ADCs whose sampling rates cannot scale to meet this demand. Moreover with each bit of increased resolution comes increased power consumption, cost and complexity [19]. Compressed Sensing (CS) has emerged as a framework that can decrease signal acquisition cost at the sensing stage by operating on a small set of non-adaptive, linear and mostly randomized measurements resulting in acquisition and compression at the same time. CS relies on the fact that most signals in nature are sparse in a certain domain. This means that they can be represented by a reduced set of coefficients (say K) in that domain. Then the sparsity of the signal is said to be K.

The standard CS framework entails recovering a signal x of size N from measurements y of size $M << N$ which are obtained by using $y = \phi x$ where ϕ is the CS matrix of size M x N. The solution involves design of the measurement matrix ϕ such that the linear dimensionality reduction from $x \in \mathbb{R}^{\mathbb{N}}$ to $y \in \mathbb{R}^{\mathbb{M}}$ does not affect the recovery of important information of the signal x and also allows the reconstruction algorithm to get back x from as low as possible number of measurements.

CS has been the major motivating force in many real-world applications involving data compression and acquisition, channel coding and inverse problems [7]. The most popular ones in the circuits and systems community are the single-pixel camera [12] and the Analog-to-Information converter [11].

1.3 Interference cancellation in the frequency domain

As stated in Section 1.1 above, the main problem is the presence of nonlinearities in the front-end which significantly influence the interference mitigation. In the new system that is developed in this thesis, as shown in Figure 1.1, the sensing stage is moved in front of the LNA to protect the system from the inherent nonlinearity. This might increase

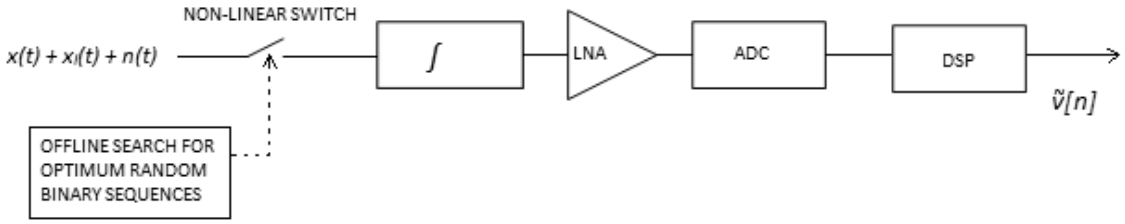

Figure 1.1. Block diagram of a single branch of the receiver envisioned: $x(t)$ is the weak message signal buried under strong interferer $x_I(t)$ and $n(t)$ is the noise. The goal is to make $\tilde{v}[n]$ interference-free and achieve efficient CS reconstruction. Under the proposed method $\phi_i(t)$ is obtained from the offline search block

the noise figure of the system on the whole, but it can be compensated by gain in the reconstruction, which is demonstrated in Chapter 3. Our goal is to make use of zeros or nulls in the frequency domain to create the opportunity for interference mitigation right at the sensing stage of the receiver. The measurement matrix ϕ is implemented by using projection waveforms $\phi_i(t)$. Since the design of these waveforms is not arbitrary in view of the hardware implementation, we consider binary sequences as they have the potential to form very good CS matrices and their implementation in hardware is simple and viable. The design of these sequences such that they cancel narrowband interference forms the core problem in this thesis. This problem reduces to a random search for good sequences, the analyses of which is the main topic considered here.

1.4 Contribution

It will be proved with simulation results that interference cancellation methods cannot be designed by ignoring nonlinear front-end blocks. Also a new mitigation method will be proposed as an alternative to this which uses spectral nulls to cancel out the interferer before entering the LNA of the receiver. But when binary sequences are used for the proposed method, it is non-trivial to obtain sequences that will help in nulling out the interferer and thus a substantial amount of search is required. The major contribution of this

thesis is an analytical approach to estimate the probability of occurrence of nulls in binary sequences. This can then be used by the system designer to choose appropriate system parameters without initiating a large number of futile (and costly) searches. The use of binary sequences in the presence of nonlinear LNA will be investigated and compared with OPM.

This thesis is organized as follows: an outline of compressed sensing results is given in the Chapter 2, followed by Chapter 3 where the description of the wideband interference problem, the demerits of previous CS-based approach and the description of the proposed method using ideal switches will be detailed accompanied by appropriate simulation results. We will look at the search methods associated with switch sequence design and results indicating their performance in Chapter 4.

CHAPTER 2

COMPRESSIVE SENSING BACKGROUND

Sparsity provides a way to compress acquired information and helps to improve the efficiency of data acquisition protocols. It leads to dimensionality reduction and efficient modeling. As typical signals have some structure, they can be compressed efficiently without much perceptual loss. For example, JPEG2000 exploits the fact that many signals have a sparse representation in a fixed basis, meaning that one can store or transmit only a small number of adaptively chosen transform coefficients rather than all the signal samples. Acquiring the full signal, computing the complete set of transform coefficients followed by encoding the largest coefficients and discarding all others is a wasteful process of massive data acquisition followed by compression. If it would be possible to acquire the data in already compressed form, the efficiency of data acquisition would potentially be vastly improved. Compressed sensing has evolved from these thoughts.

Taking the example of wideband radio frequency signal analysis, we may only be able to acquire a signal at a rate which is much lower than the Nyquist rate. Because of the current limitations in ADC technology, this motivates CS as a wideband signal acquisition protocol in communications, as CS can sample less with a non-adaptive nature and yet still reconstruct signals accurately. Using CS-based architectures in place of costly and cumbersome ADCs is very rewarding in the sense that we can sample much lower than the Nyquist rate [11] and potentially reconstruct the signal as good as the reconstruction performed by Nyquist rate ADCs. It needs to be pointed out that CS measurements are sometimes affected by pre-measurement noise, whence resulting in a phenomenon called noise-folding which impacts the SNR (signal to noise ratio) of the signal/vector to be recovered signif-

icantly if the pre-measurement noise is large enough. But it has been proved that even in the presence of pre-measurement noise, CS results hold up well [8].

Fundamental premises:

A signal x is said to be k-sparse if its support $\{i : x_i \neq 0\}$ is of cardinality less than or equal to k. For example a signal which is dense in the time domain (or continuous) might be represented completely by a highly reduced set of samples in the Fourier domain. Similarly we can discard most of the coefficients of an image when it is represented in the DCT (Discrete Cosine Transform) domain due to the fact that most of its visually perceptible features are present in a small set of non-zero coefficients.

Speaking in general terms, the reconstruction problem can be stated as: build a vector $x \in \mathbb{R}^{\mathrm{N}}$ by acquiring linear measurements y about x of the form

$$y = \phi x \tag{2.1}$$

where y is the vector of compressive measurements acquired of the original signal x and $y \in \mathbb{R}^{\mathrm{M}}$ and ϕ is an MxN matrix. If the matrix ϕ has orthogonal columns, then x can be recovered by using $\phi^{-1}y$. But we are concentrating on low-rate sampling methods with the size of ϕ being M by N where $M \ll N$. Then the recovery using (2.1) becomes an insufficiently posed inverse problem. If x is k-sparse, then it is possible[1, 2] to reconstruct the whole signal by solving a convex optimization problem:

$$\tilde{x} = \arg\min_{x \in \mathbb{R}^{\mathrm{N}}} \|x\|_1 \quad \text{subject to} \quad y = \phi x \tag{2.2}$$

where $\tilde{x}$ is the reconstructed signal and $\tilde{x} \in \mathbb{R}^{\mathrm{N}}$.

2.1 Sensing matrices

Let $x(t) = \sum_{i=1}^{n} \alpha_i \psi_i(t)$, where ψ is the matrix with columns ψ_i which are mutually orthogonal and ψ is a basis in which x can be sparsely represented with no more than k

non-zero coefficients. If x is represented in its sparsity basis ψ, we can express it as $x = \psi\alpha$ or $\alpha = \psi^* x$. Let us introduce a matrix A here of size M by N such that $\phi = A\psi$ and so write $y = Ax$. For recovery from small number of measurements to be possible in CS, the matrix A needs to be incoherent or uncorrelated with ψ. Coherence can be referred to as the largest correlation between any two elements of A and ψ. Now, the coherence μ between A and ψ can be defined as follows,

$$\mu(A, \psi) \equiv \sqrt{n} \cdot \max_{1<k,j<n} |\langle A_k, \psi_j \rangle| \tag{2.3}$$

and is bounded as $1 \leq \mu(A, \psi) \leq \sqrt{n}$. For compressed sensing, the structured matrix A needs to be chosen such that it is maximally incoherent with ψ which means that the value μ should be as close to 1 as possible. When $A = \psi$, $\mu = \sqrt{n}$ and the coherence is maximized, which means no compressed sensing is possible.

2.2 Null space conditions

To have the ability to recover all sparse vector x from the observation A, the null space $\mathcal{N}(A)$ of matrix ϕ must not contain any vectors in the set $\sum_{2k}$ of all $2k$-sparse vectors. The null space property quantifies the fact that any vector in the null space of matrix ϕ should not be too concentrated on a small subset of indices.This also holds for any recovery algorithm using a sensing matrix ϕ. For a matrix of null space property of order k, it should hold

$$\|h_\Lambda\|_2 \leq C \frac{\|h_{\Lambda^c}\|_1}{\sqrt{k}} \tag{2.4}$$

where h_Λ denotes any vector $h \in \mathcal{N}(\phi)$ with indices corresponding to all Λ[1] such that $|\Lambda| \leq k$ [6] for some constant C.

So, if h is exactly k-sparse there exists Λ such that $\|h_{\Lambda^c}\|_1$ = 0 which means the only k-sparse vector in the null space of ϕ will be $h = 0$ from the above relation.

[1] Λ is such that $\Lambda \subset \{1, 2, 3...N\}$ and let Λ^c be the complement of Λ which is $\{1, 2, 3...N\}$ - Λ

2.3 Restricted Isometry Property

The construction of the sensing matrix needs to be done according to the Restricted Isometry Property (RIP) which is defined as follows: for $\delta \in$ (0,1) and for all $x \in \sum_k$

$$(1-\delta)\|x\|_2^2 \leq \|\phi x\|_2^2 \leq (1+\delta)\|x\|_2^2 \tag{2.5}$$

where δ is called RIP constant. This property can be explained as follows: if ϕ is an orthogonal matrix, then ϕ is an isometry, and δ = 0 for any k, which is the best possible constant. Increasing the number of rows to a matrix ϕ will improve (i.e., decrease) its RIP constant. When the above property holds, ϕ approximately preserves the Euclidean length of k-sparse signals, which in turn implies that k-sparse vectors cannot be in the null space of ϕ. A parallel explanation of the RIP is to say that all subsets of k columns taken from ϕ are nearly orthogonal. The columns of ϕ cannot be exactly orthogonal since there are more columns than rows. Let δ_{2k} denote the RIP constant concerning the reconstruction of a $2k$-sparse signal. Suppose that δ_{2k} is sufficiently less than one. This implies all pair-wise distances between k-sparse signals must be well preserved in the measurement space. If x_1 and x_2 are 2 distinct k-sparse signals, the RIP becomes,

$$(1-\delta_{2k})\|x_1 - x_2\|_2^2 \leq \|\phi(x_1 - x_2)\|_2^2 \leq (1+\delta_{2k})\|x_1 - x_2\|_2^2$$

For a different perspective assume $\delta_{2k} = 1$; this implies

$$\phi(x_1 - x_2) = 0$$

and the measurement vector y is the same for two distinct signals x_1 and x_2. Therefore, for any recovery algorithm, the choice of measurement matrix should be such that $\delta_{2k} < 1$.

Theorem 1. *(Theorem 1.8 of [6]) Suppose that ϕ satisfies the RIP of order $2k$ with $\delta_{2k} < \sqrt{2} - 1$ and we obtain measurements of the form $y = \phi x$. The solution $\tilde{x}$ to* (2.2) *obeys*

$$\|\tilde{x} - x\|_2 \leq C_0 . \frac{\sigma_k(x)_1}{\sqrt{k}}$$

This theorem states that one can recover a k-sparse signal x exactly provided ϕ satisfies RIP.

Recovery of compressible signals:

Signals or vectors may not be always sparse, but they can be compressible meaning they can be well-approximated by a sparse signal. These are referred to as compressible or near-sparse signals. For a compressible signal x we can estimate the level of compressibility by finding the error in comparison with any sparse signal $\tilde{x} \in \sum_k$ by the L_p norm,

$$\sigma_k(x)_p = \min_{\tilde{x} \in \sum_k} \|x - \tilde{x}\|_p \tag{2.6}$$

If $x \in \sum_k$ then it means $\sigma_k(x)_p = 0$ for any p. A common assumption is that the coefficients of the signal $\tilde{x}$ though not exactly sparse in a transform domain, might have coefficients that decay according to a power law. In particular consider $x = \psi\alpha$ and sort the coefficients α_i such that $|\alpha_1| \geq |\alpha_2| \ . \ . \ . \ . \geq |\alpha_n|$. Then, it can be said that the coefficients obey a power law decay if there exist constants C_1, q such that,

$$|\alpha_i| \leq C_1 i^{-q}$$

As q increases, the coefficients α decay faster and so the compressible signal x can be represented accurately using only $k \ll N$ coefficients [6].

2.4 Signal recovery in the presence of noise

As stated in (2.2) the k- sparse signal x can be recovered using $L1$-norm minimization under the measurement matrix conditions explained in previous sections. But the same

method of recovery cannot be applied when the signal or vector contains noise, that is $y = \phi x + n$ with n being the noise in the measurements. However, an extension to the algorithm (2.2) can be used which can be stated formally as,

$$\tilde{x} = \arg\min_{x \in \mathbb{R}^N} \|x\|_1 \quad \text{subject to} \quad \|y - \phi x\|_2 \leq \epsilon \tag{2.7}$$

where $\epsilon \geq \|n\|_2$ and this method is known as Basis Pursuit with Denoising(BPDN).

Theorem 2. *(Theorem 1.9 of [6]) Suppose that A satisfies the RIP of order $2k$ with $\delta_{2k} < \sqrt{2} - 1$ and let $y = \phi x + e$ where $\|e\|_2 \leq \epsilon$. The solution $\tilde{x}$ to* (2.7) *obeys*

$$\|\tilde{x} - x\|_2 \leq C_0 \frac{\sigma_k(x)_1}{\sqrt{x}} + C_2 \epsilon$$

where

$$C_0 = 2\frac{1 - (1 - \sqrt{2})\delta_{2k}}{1 - (1 + \sqrt{2})\delta_{2k}},\ C_2 = 4\frac{\sqrt{1 + \delta_{2k}}}{1 - (1 + \sqrt{2})\delta_{2k}}.$$

This theorem gives a guarantee for deterministic measurement matrices, but it is a problem of combinatorial complexity to verify the RIP for a given deterministic matrix. Random matrices with a fixed number of rows M have very good RIP constant δ_{2k} with high probability.

2.5 Sensing matrices that satisfy RIP

We need to design a sensing matrix that can recover all N entries of x using M measurements. To maintain orthogonality of a matrix ϕ with more columns than rows means that for a given structured matrix ϕ, we would need to verify the orthogonality each of the $\binom{N}{k}$ different combinations of sub-matrices (for recovery of k-sparse signals). Randomizing the matrix entries has been the key step towards building effective measurement matrices in Compressed Sensing. A matrix A whose entries are drawn in an independent and identically distributed manner from a random distribution has been proven to obey the

RIP with high probability [3]. Gaussian, Bernoulli and generally any sub-Gaussian distribution can be used for this purpose. Mathematically, it has been shown that A obeys the RIP of order $2k$ with constant δ_{2k} with probability atleast $1 - 2 \cdot \exp\left(-c_1 \delta_{2k}^2 M\right)$ where c_1 is a constant, if the entries of ϕ are chosen according to such distributions and the number of rows M of ϕ is

$$M \geq k \log(n/k)/\delta_{2k}^2 \text{ [6]} \tag{2.8}$$

2.6 Orthogonal Projection Method

CS has motivated application in interesting scenarios. One such has been interference rejection where the measurements are made away from the interference subspace when it is known that interferer and desired signal are both sparse in the same domain. The basic premise is to build an orthogonal operator P such that when the measurements y are multiplied by P such that the product $P\phi$ obeys the RIP [15], that is $Py = P\phi x = P\phi(x_S + x_I) = P\phi x_S$ where x_S is the desired signal and x_I is the inteferer. The design of the method is such that the spectral components of the interference will be in the nullspace of the projection matrix or operator, P. The construction of the operator depends on the knowledge of the interference. Let ϕ_J denote the matrix formed by indexing the columns of ϕ by a set J. Assuming an identity basis for the sparsity domain of x_I, if J is the set of indices corresponding to the position of one in each of the basis vectors, then product ϕx_I will lie in the range of ϕ_J, $\mathcal{R}(\phi_J)$. Then, the operator P is built such that its nullspace is equivalent to range $\mathcal{R}(\phi_J)$ [15].

An implementation of P is given in [15] as,

$$P = I - \phi_J \phi_J^{\dagger}, \text{ where } \phi_J^{\dagger} \text{ is the pseudo-inverse of } \phi_J$$

and pseudo-inverse is evaluated as, $\phi_J^{\dagger} = (\phi_J^* \phi_J)^{-1} \phi_J^*$.

This method of interference cancellation will be referred to as Orthogonal Projection Method in this thesis. In the Chapter 3, the performance of the receiver where this scheme is employed will be analyzed under linear and nonlinear front-end scenarios.

CHAPTER 3

SWITCH SEQUENCE DESIGN

In this chapter, we will look at the design of rows of the measurement matrix ϕ with a goal towards easily implementing them in hardware. As stated in Chapter 2, a matrix made of elements drawn from i.i.d. Bernoulli distribution can form a very good CS measurement matrix and also can built in hardware with the use of switches.

First, we will look at some of the important aspects concerning wideband receivers, potential examples of interference and the problems associated with interference mitigation using compressed sensing proposed prior to this project.

3.1 Design aspects for wideband receivers

Futuristic communication systems based on promising areas such as software radio, cognitive radios unlike the present RF receivers would need to receive any modulation across a large frequency spectrum using a wideband RF front-end module with several GHz bandwidth. The system starts initially with a wide bandwidth suited for a gamut of applications and then down-selects in a reconfigurable way the required narrow bandwidth signals which can then be digitized with a low power ADC. As stated earlier the presence of interference is ubiquitous, especially in wireless systems. Nonlinearities in the analog front end make the interference significantly harmful, predominantly when the desired signal is weak. Detection of weak wideband signals in the presence of interference also faces the problem of inadequate quantization due to limited dynamic range of ADCs. Low-cost ADCs cannot simultaneously offer both high sampling rate and high quantization resolution [19]. Attempts to solve these problems until now have focussed on mitigating the interferer

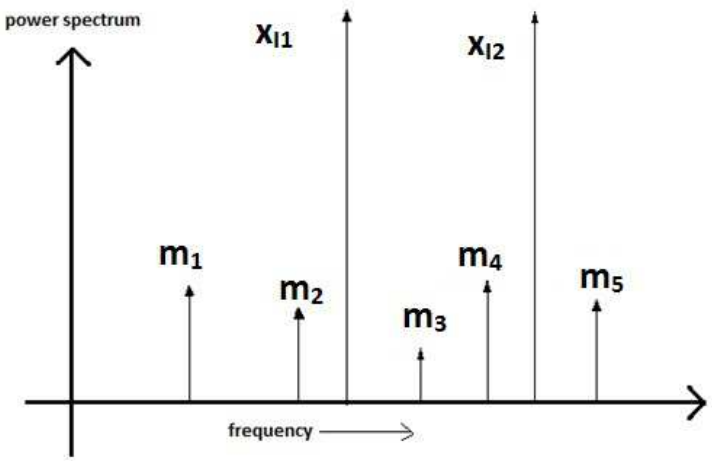

Figure 3.1. Presence of interference in a wideband spectrum, where X_{I1} and X_{I2} represent interferers in the same band as message signals $m_1 - m_5$

following the analog front end where there is combination of low noise amplifiers(LNAs) and down conversion mixers.

3.2 Examples of interference

WiFi[1] networks (802.11 b/g/n/ac) are the major victim of interference effects from devices like cordless telephones which use the 2.4 GHz frequency band as does the WiFi network [23]. This can easily cause a reduction in data rates or complete jamming of WiFi signals whenever a phone conversation takes place. The microwave oven and video senders like CCTV (closed circuit television) cameras are also sources of interference for WiFi channels as they operate in the same band as WiFi. Though the microwave oven signals have poor shielding, their duty cycle is less than 50 percent which has helped in making WiFi signals to adapt accordingly and prevent interference. Video senders have 10MHz bandwidth and use bands adjacent to WiFi channels, and often are closer to the receiver and hence become high power interference to WiFi. This results in high packet

[1]Wireless Fidelity (IEEE 802.11 standard)

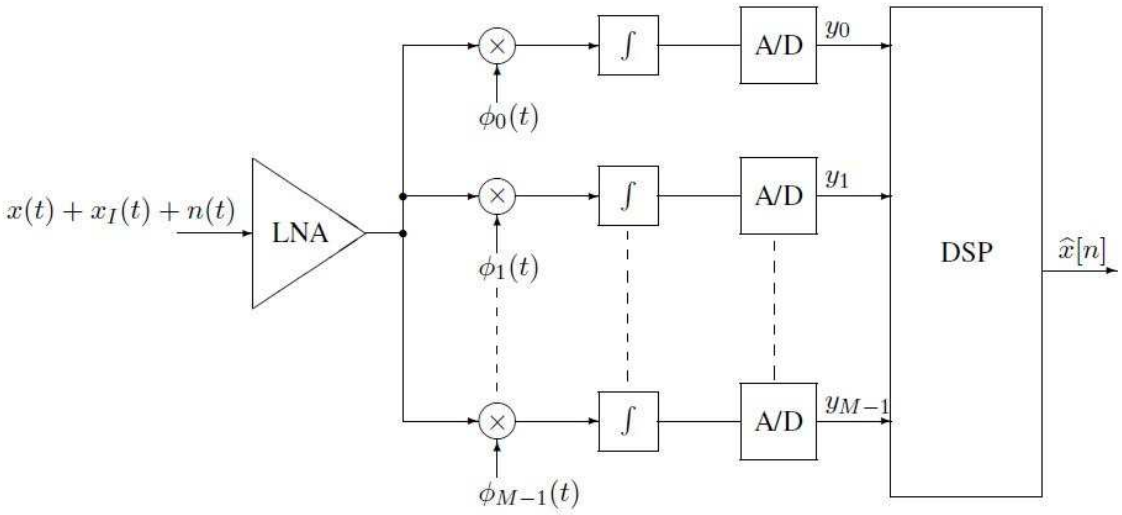

Figure 3.2. Block Diagram of a prototypical wideband receiver.

loss, decrease in throughput and lowering of receiver sensitvity [23]. These effects become prominent considering the gamut of applications of future receivers have to cater to.

The numerous unused free channels available in the range of operation of US TV stations can be used for cognitive radios. But the adjacent channels might have signals at much higher power which can become powerful blocker signals and reduce the dynamic range of receivers using the free space. A second band of interest might stretch from 800 MHz to 6 GHz where GSM[2], WCDMA[3], WiMAX[4], WLAN[5] signals co-exist and can be interferers [18]. The strongest is GSM at 900MHz. The signal level received at one meter from a GSM handset is of the order of 1mW, whereas a cognitive radio in an adjacent channel would need to be able to receive signals with power less than 1pW. Although the interferers are at different frequencies than the white space channels, nonlinearities in the initial stages

[2]Global system for mobile communications

[3]Wideband code division multiple access

[4]Wireless interoperability for microwave access

[5]Wireless local area connection

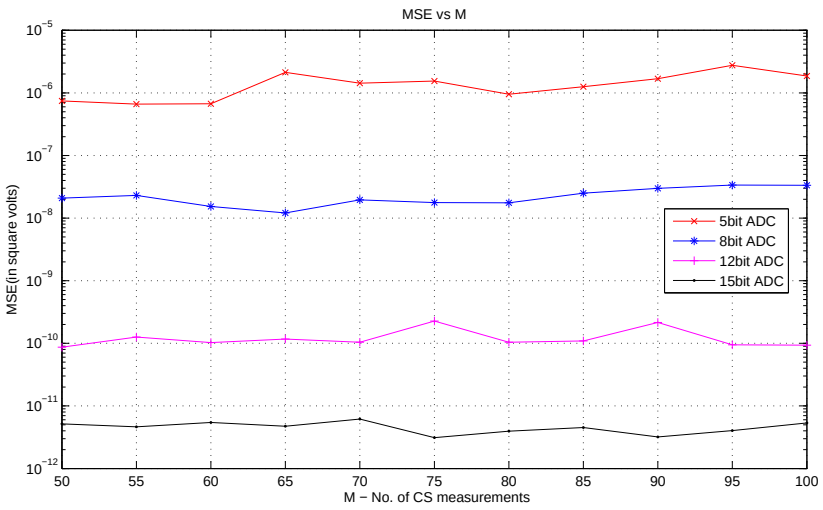

Figure 3.3. Performance of Orthogonal Projection Method (OPM) using different ADCs to analyze the effect of ADC bit resolution on the reconstruction when OPM is used. For this simulation, an interference of 80dB with a linear front end was used.

of the wideband receiver cause the larger signals to distort, or block, the smaller signals. The presence of LTE-TDD[6] and LTE-FDD[7] bands (downlink as well as uplink) very close to WiFi channels calls for strict co-existence rules to prevent such kind of interference and out-of-band noise.

3.3 Sparse measurement matrices

Inference can be drawn from [5] about measurement sparsity which means using matrices with zeros present in each row for compressed sensing. It gives sharper bounds on the number of measurements required for good recovery for Gaussian or sub- Gaussian measurement matrices with dense rows when compared to standard compressed sensing results.

[6]Long term evolution - time division duplex

[7]Long term evolution - frequency division duplex

The choice of using Gaussian measurement ensemble in compressed sensing produces highly dense matrices, which may lead to very high computational complexity and storage requirements. Impressively, sparse measurement matrices can also lead to fast decoding algorithms by using problem structure at the same time reducing demand on storage and processing hardware. The downside though is measurement sparsity can potentially reduce statistical efficiency by requiring a higher number of measurements to recover the signal. By intuition the nonzeros in the signal may rarely align with the nonzeros in a sparse measurement matrix. We will try to leverage this idea of using sparsity in the measurement matrix to overcome some of the problems associated with interference cancellation using compressed sensing.

3.4 Interference cancellation using compressed sensing

3.4.1 Previous approaches to the problem

Compressed sensing has been used to remove interference under the assumption that the subspace in which interference is sparse is known. This knowledge helps us to project the compressive measurements orthogonally to this subspace thereby eliminating interference completely [15]. This method, though very effective, needs to be implemented in the DSP as it operates on the digital samples of input signal. This approach, referred to as Orthogonal Projection Method (OPM) in this thesis has been introduced in the Chapter 2.

We know that in a receiver the front end is composed of the ADC and LNA apart from the IF stages. The dynamic range of the receiver is dictated by the ADC effectively. If there is a high power interferer in the frequency band being operated upon, the weak message signal will get buried due to the power difference. Nonlinearities in the front end combined with the presence of interference create additional signals at frequencies that are not just harmonics of the interferer but also at sums and difference frequencies of the interferer with the message signals. These are referred to as intermodulation(IM) products. In this situation, proper digitization cannot be possible and subsequently the DSP cannot recover

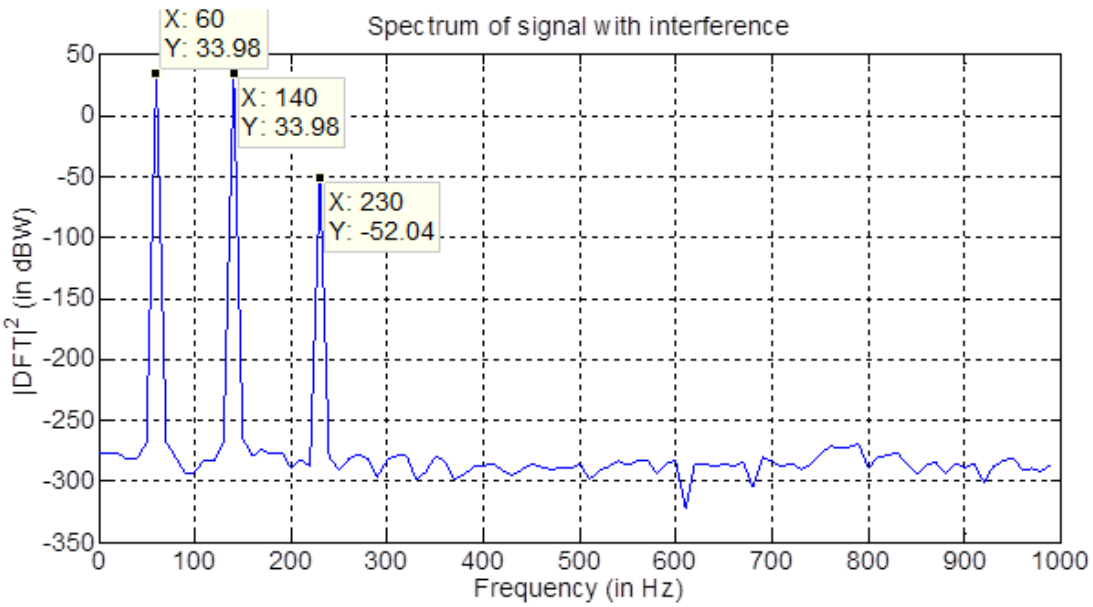

Figure 3.4. Spectrum of receiver band of interest with two inteferers at about 80 - 90dB higher than the single frequency message signal. We give this as input to LNA to understand the effect of nonlinearities. Details for the figure (a) message signal is $5\text{x}10^{-6}\sin(2\pi 230t)$ (b) interferer signals are $0.1\sin(2\pi 60t)$ and $0.1\sin(2\pi 140t)$ (c) Non-linear model used: if y is output of amplifier and x is the input, then $y = 10x - 10x^3$ (d) For the y-axis, we take $10\log_{10}(|DFT|^2)$ (DFT is Discrete Fourier Transform)

.

the input message signal reliably. The performance of OPM using values of commonly used low-power ADCs with a linear front end has been shown in the Figure 3.3 and it can be seen we need completely linear front end along with a high dynamic range ADC to extract good performance for this linear scheme.

A prototype of a wideband compressive receiver [17] was built based on [11] and [15]. While this offers a way to cancel interference using compressed sensing, the main drawback of this architecture is the comfortable omission of nonlinear front end.

The block diagram of the prototypical compressive receiver is shown in Figure 3.2 where the front-end consists of the LNA, sensing branches and ADC, followed by the backend DSP. Often the signal received is extremely weak necessitating the LNA in the

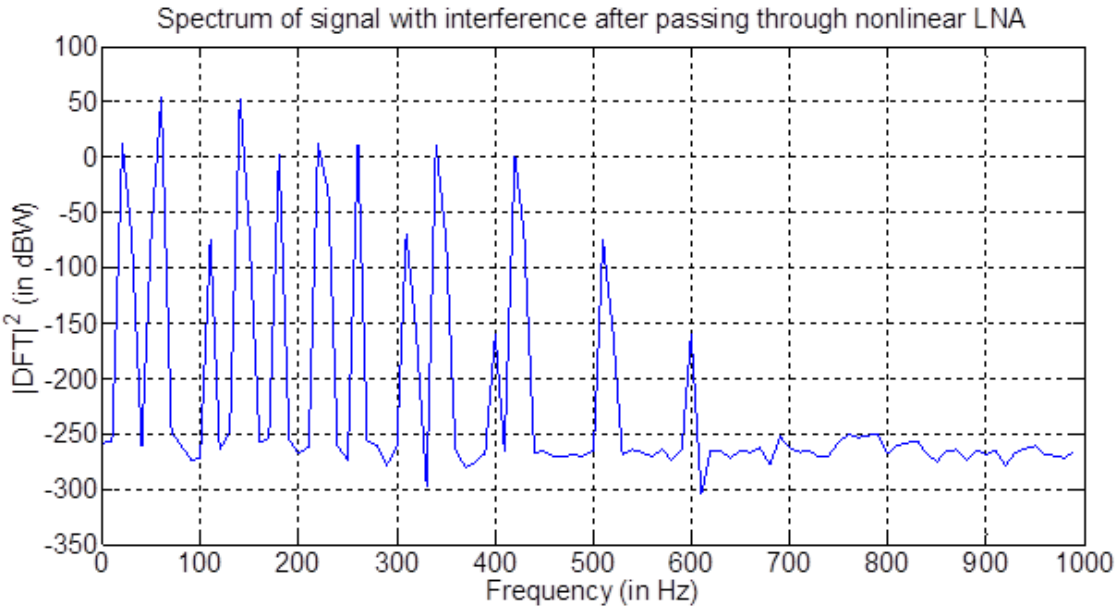

Figure 3.5. Spectrum at the output of LNA with the assumed nonlinear model. As shown the band of interest is corrupted by intermodulation products and harmonics.

front end. The input signal consists of the message signal $x(t)$ with added noise $n(t)$ due to channel variations and distortions and the interference $x_I(t)$. The mathematical model for the nonlinear LNA assumed in this thesis is:

$$y(t) = k_1 m(t) + k_3 m^3(t) \tag{3.1}$$

where $y(t)$ is output of LNA and $m(t)$ is input and the parameters used are $k_1 = 10$ and $k_3 = -10$.

As it can be seen there is a 3^{rd} order term in the LNA which results in intermodulation products in $y(t)$. Let us consider the signal $m(t) = 5{*}10^{-6}sin(4t){+}0.1sin(5t){+}0.1cos(3t)$ with the last two terms being the interferers. Substituting this in (3.1) and expanding the terms would result in harmonics(integer multiples), sum and difference products in which the most problematic one would be a 3^{rd} order interferer right on top of the message signal frequency. We note here that the amplitude of message signal in this model is orders of

magnitude lesser when compared to that of the interference. The power level of interference $x_I(t)$ to message $x(t)$ ratio is about 90dB. The effect of the harmonics and IM products is illustrated in the Figures 3.4 and 3.5. When $m(t)$ becomes input in the block diagram of receiver shown in Figure 3.2, inserting the model of ideal LNA of (3.1), it becomes evident that the two interferers and the message signal form many IM products as shown in Figure 3.5 which give rise to unnecessary additional signals in the receiver bandwidth making the task of interference cancellation quite challenging. It can be seen that the IM products are at a significantly higher power compared to the message signal. The method of [15] will not be useful in such a situation. This is due to the fact that when using OPM, we are projecting away from the interferer subspace which only cancels out the interferer signal but not the IM products and harmonics.

3.4.2 Interference mitigation inspired by Frequency domain perspective using non-linear switches

The knowledge of environment or of common interferers can be leveraged to develop algorithms for interference cancellation using structured sparsity models accounting for nonlinearity of analog-to-information converter.

One of the branches of block diagram of the new receiving system proposed is given in Figure 1.1. Let $x(t) + x_I(t) + n(t)$ be denoted by $m(t)$ which is the input to the receiver branch and $\hat{v}[n]$ is the interference-free digital output of the DSP. This design does not have the LNA as the first block in the receiver and so we can create the possibility of cancelling the interferer before it reaches the LNA. This might increase the noise figure of the circuit as a whole, but this can be compensated by the impressive gain in terms of interference mitigation as shown in Figure 3.6. The sensing consists of M branches with a mixer and integrator. The design for the simulations done for Figures 3.6, 3.7 is such that we hope to achieve many interference-free branches by placing random zeros in the frequency domain of the measurement vectors.

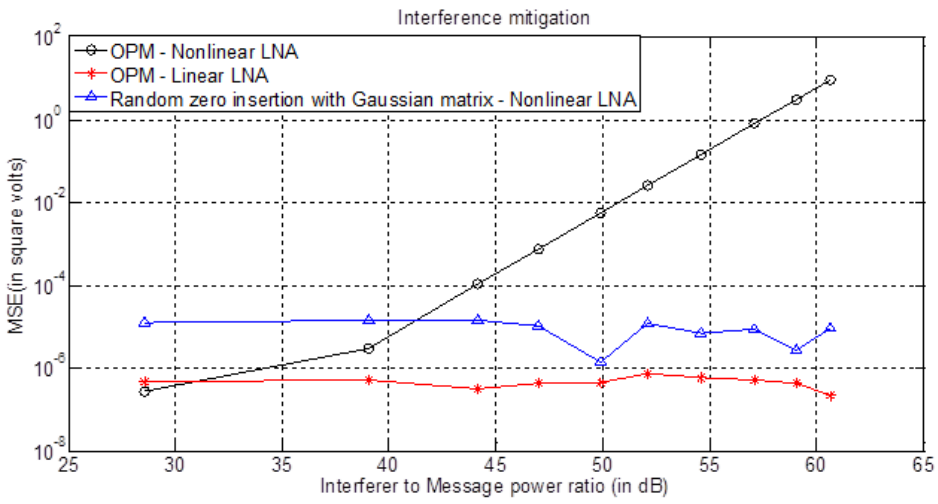

Figure 3.6. Mean-squared error (MSE) in the reconstructed signal as a function of the interferer-to-signal power. The graphic shows how OPM fails when an non-ideal LNA is used and under the same conditions, the proposed method works well. Details: (1) an OPM interference suppression approach with a more accurately modeled (nonlinear) LNA in the RF front-end, (2) OPM interference suppression approach [15] with a linear RF front-end and (3) proposed method under same model of nonlinear LNA following the switches (assumed ideal here) used for interference rejection. The signal-to-noise ratio (SNR) is 30 dB, the signal length is $N = 1000$, the message signal has sparsity $k = 5$ in the frequency domain, the number of measurements is $M = 125$ and the interferer is narrowband (one-dimensional or single-tone). The average message signal amplitude is 0.5mV and interferer ranges from about 1mV to 1V. The nonlinear model of (3.1) has been used for the LNA for this plot. The measurement matrices are drawn in an independent and identically distributed (i.i.d.) manner from a Gaussian distribution for all schemes with the proposed method randomly zeroes 40% entries in the frequency domain. Basis Pursuit with Denoising (BPDN) is used for signal recovery in each case.

Measurement projection corresponds to random filtering of observed signal that zeroes a certain set of bands. These branches can be determined and used for the measurement matrix design in the subsequent compressive signal processing. The projections are created by multiplying a time windowed version of input message signal with vectors generated from nonlinear switches. Being drawn i.i.d. from a random distribution facilitates the RIP maintenance of the columns of the final measurement matrix. We know according to Parseval's theorem that:

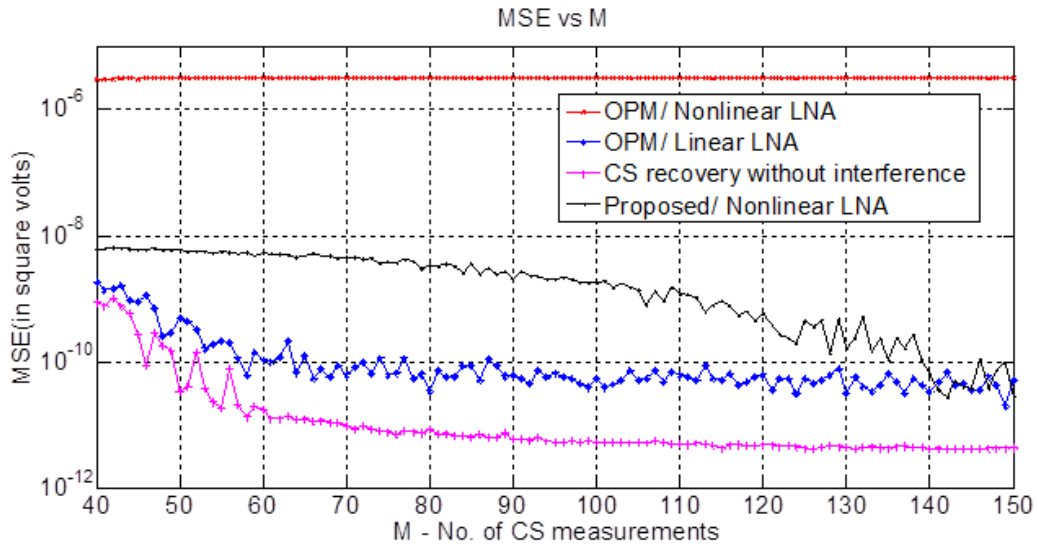

Figure 3.7. Mean-squared error (MSE) in the reconstructed signal as a function of the number of CS measurements/projections. The details are same as in the Figure 3.6 except (1) the interference to message power is kept constant at 85dB (2) N = 500 (3) message signal amplitude is 5uV (micro volts) and interferer is at about 0.1V. The plot referred to as 'CS recovery without interference' is the scenario where there is no interferer in the system and so results in the best MSE. It is helpful for comparing both OPM and proposed method.

$$\int r(t) \cdot h(t)dt = \int R(f) \cdot H^*(f)df$$

where $R(f)$ and $H(f)$ are the Fourier Transform of $r(t)$ and $h(t)$ respectively and $H^*(f)$ is conjugated version of $H(f)$. So from this result and from the fact that each measurement is an inner product of measurement vector $\phi_i(t)$ with the message signal $m(t)$, it is same as multiplying in the frequency domain with the conjugated version of Fourier transform of corresponding vector.

Now it can be seen that the insertion of zeros in frequency domain directly helps in cancelling interference in message signal when the location of nulls coincides with frequency location of the interferers. Although the presence of interference affected branches is quite possible, due to the fact that the interference can be detected in the branches with unusually high values, we can selectively use only those branches that are interference-free and recover the message signal using the CS-based algorithms in the subsequent DSP. Intuitively,

we would need more branches in this method than OPM, which can be compensated by the gain in interference cancellation shown in Figure 3.7. The generation of the binary sequences with the required properties is considered separately in the next chapter.

It can be seen that OPM works well until when are no prominent IM signals. When the interferer is strong enough to cause severe IM products and harmonics, the technique ceases to be effective and there is almost exponential subsequent increase in the mean square error. On the other hand, the same technique works well for an ideal front-end (linear LNA) which can be seen the Figure 3.6. The proposed method shows very good performance even in the presence of nonlinear LNA as seen in the same figure.

The Figure 3.7 shows the comparison of the OPM and the proposed method under the conditions of a nonlinear front end and a linear front end, operated on the interference power ratio of 80dB and LNA mathematical model previously assumed. An infinite amount of dynamic range was assumed for both the schemes. Each branch in the receiver refers to one CS measurement. It can be seen that, increasing the number of branches has no effect on OPM for a nonlinear front end with a high MSE depicting complete failure of reconstruction. But the same scheme under a linear front end does perform almost close to the CS recovery without any interference. On the contrary the proposed scheme shows remarkable improvement with the increase in the number of branches in the sensing system and almost converges to OPM under linear front end and CS without interference at around 30 times the sparsity.

Hence this would require that the rows in the measurement matrix need to have a number of nulls in their frequency response to aid in the cancellation of interferer at sensing stage itself. If the choice was not important we could use a Gaussian measurement matrix. The steps are:

1. Design the Gaussian matrix in frequency domain

2. Insert zeroes randomly in each of its rows

3. Take IFFT[8] of each row

4. Assuming the branches where interferer is cancelled can be distinguished, use rows corresponding to these branches in sensing and recovery.

Using mixers for this purpose involves 2 problems. Mixers are nonlinear at large bandwidths and are difficult to build if $\phi_i(t)$ has amplitude modulation. We know that random binary sequences form very good measurement matrix choice in terms of maintaining RIP of the measurement matrix ϕ and minimum number of measurements required to reconstruct the signal from its projections onto the binary vectors. These are also easy to be generated in hardware using switches, bringing our interference cancellation scheme closer to hardware.

To state formally, our core design problem is to design a collection of long binary sequences whose discrete Fourier transform contains a lot of spectral nulls to facilitate interference cancellation before entering nonlinear blocks of receiver.

[8]Inverse Fast Fourier Transform

CHAPTER 4

SWITCH SEQUENCE SEARCH

The problem of interference cancellation in this thesis comes down to finding random binary sequences that exhibit the unique property of having many nulls in their frequency domain. From the system setup described in the Chapter 3 in the Figure 3.2, the i^{th} branch calculates the projection on the vector $\phi_i(t)$ by $y_i = \int_0^T u(t)\phi_i(t)dt$ where $u(t) = x(t) + x_I(t)$ (This is linear due to the fact that we placed the LNA after the switches in our architecture). From Parseval's theorem, we know that having nulls in the frequency response of $\phi_i(t)$ facilitates the filtering of interferer components of $u(t)$. Due to a simpler hardware implementation, the projection vectors are generated by periodic on-off switching instead of a mixer, as stated previously in Chapter 3. Then $\phi(t)$ can be written as,

$$\phi_i(t) = \sum_{j=0}^{N-1} b_j^{(i)} p(t - jT_s), \tag{4.1}$$

where $b_j^{(i)} \in \{0, 1\}$, and $p(t)$ is a square pulse of width T_s and N is the dimensionality of the signal to be reconstructed. Define a binary sequence $\mathbf{b^{(i)}} = [b_0^{(i)}, ..., b_{N-1}^{(i)}]$. The problem of finding the optimum set of random binary sequences can be characterized as:

$$\mathbf{b}_{opt} = \text{argmax}_{\mathbf{b}\in\{0,1\}^N} f(b) \tag{4.2}$$

where $f : \{0, 1\}^N \rightarrow R$ is the objective function that measures how good the sequence b is in terms of interference cancellation. The problem given in (4.2) is called as pseudo-Boolean optimization problem. It can be viewed as the problem of finding an optimum object from a finite set of objects. It can be seen that brute force search is not feasible

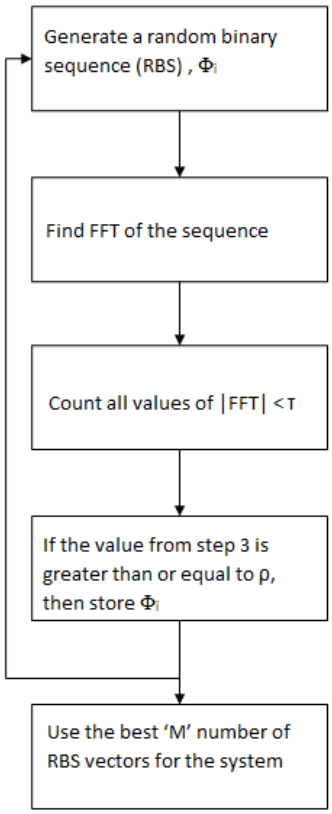

Figure 4.1. Steps in the search algorithm. The best M rows refer to those that have spectral nulls at the interferer frequency. Details for the parameters: (1) τ : The threshold which defines whether a $|DFT|$ bin is a null (2) ρ : The number of spectral nulls of a binary sequence (3) M: Number of measurements or number of rows of measurement matrix, ϕ (4) N: size of the sequence

for even nominal values of N, as it would be very difficult due to the size of the search space $S = \{0, 1\}^N$. In this thesis, we try to search for a collection of good sequences with emphasis on finding specifically sequences exhibiting the property of many spectral nulls.

4.1 Sequence generation procedure

The approach is to generate the optimum random binary sequences off-line and use them for the collection of measurements. The pool size S is the span of the search space that we use to generate the required sequences for the matrix ϕ. It is needed that we obtain

sequences that exhibit the property of having many spectral nulls. In order to define a null, a threshold needs to be chosen. Let the threshold be denoted by τ. Let the number of entries sought in the DFT of the binary sequence with magnitudes less than τ, be denoted by ρ. This can be represented by,

$$\phi_i = \{x : f_i(x) \geq \rho\}\ , x_i \in S \text{ and } S \in \{0,1\}^N \tag{4.3}$$

where $f_i(x)$ is the number of entries in the DFT of x with magnitudes less than τ and ϕ_i is the i^{th} row of ϕ.

In other words, this means sequences with at least ρ nulls in the frequency domain are needed for the system. It is understood that the selection of the parameters becomes important. The algorithm can be divided into 2 stages for the sake of analysis. First, the building up of the necessary sequences with fixed probability and size such that the presence of spectral nulls is maximized. Second, the usage of such sequences for the CS wideband system shown in Figure 3.2. In the next section the first stage is analyzed theoretically so as to form an idea about selecting the parameters for the algorithm. As S is increased, τ and ρ can be traded off to obtain much better results.

4.2 Analysis

It has been already stated that, finding binary sequences with a good number of spectral nulls forms the most important part of the interference mitigation in the receiver. With many spectral nulls, the probability of hitting the interferer increases and thus helps in interference cancellation. But finding real sequences of such nature is non-trivial and will need knowledge of how to choose parameters such as τ, ρ defined above before embarking on the search for sequences. The approach here is to model the probability of finding such sequences theoretically. This is to obtain enough information in picking τ and ρ so as to estimate the amount of search that needs to be done. We start by looking at the distribution

of the discrete Fourier transform of binary sequences. The binary sequences are modeled as shown in (4.1). Taking the DFT of ϕ_i,

$$\Omega_i(k) = \sum_{n=1}^{N} \phi_i[n] \exp(-j2\pi \frac{k}{N} n) \tag{4.4}$$

It is known that Bernoulli matrices with elements being $\{-1, +1\}$ obey the RIP with high probability [3]. But when the elements are $\{0, 1\}$ instead, RIP based results cannot be applied [22] as these matrices follow RIP for substantially higher number of rows. The number of rows is proportional to k^2 for $\{0, 1\}$ matrices as opposed to $O(k \log(n))$ when using $\{-1, +1\}$ matrices [22] [21].

If b_k is k^{th} value in the binary sequence ϕ_i , then let p = 0.5 and so P(b_k = 1) = 0.5 and P(b_k = 0) = 0.5. For this probability, the mean and variance of the real and imaginary parts of the DFT are calculated as follows:

Let Ω_R denote the random variable for the real part of the Fourier coefficients and Ω_I denote the random variable for the imaginary part.

$$\begin{aligned} \Omega(k) &= \Omega_R(k) + j\Omega_I(k), \text{ and} \\ |\Omega(k)| &= \sqrt{\Omega_R^2(k) + \Omega_I^2(k)} \end{aligned} \tag{4.5}$$

Evaluating the mean of the real part,

$$\begin{aligned} \mathrm{E}(\Omega_R(k)) &= \mathrm{E}(\sum_{n=1}^{N} x(n) \cos(2\pi n \frac{k}{N})) \\ &= \sum_{n=1}^{N} \mathrm{E}(x(n)) \cos(2\pi n \frac{k}{N}), \quad \text{moving the expectation inside the summation} \\ &= 0.5 * 0, \quad \text{as cosine sums to zero in one period (considering } k = 1, 2, 3...N-1) \\ &= 0 \end{aligned}$$

The imaginary part can also be shown to have an expectation of zero in the similar manner. Consider the variance of the random variable:

$$\sigma^2 = \mathrm{E}\{\sum_{m=1}^{N}\sum_{n=1}^{N} x(m)x(n)\cos(2\pi m\frac{k}{N})\cos(2\pi n\frac{k}{N})\}$$

$$= \mathrm{E}\{\sum_{\substack{m=1 \\ \text{when } m\neq n}}^{N}\sum_{n=1}^{N} x(m)x(n)\cos(2\pi m\frac{k}{N})\cos(2\pi n\frac{k}{N})\} + \mathrm{E}\{\sum_{\substack{m=1 \\ \text{when } m=n}}^{N} x^2(m)\cos^2(2\pi m\frac{k}{N})\}$$

Using the trigonometric identity $2\cos^2(A) = 1 + \cos(2A)$

$$= \sum_{m=1}^{N}\sum_{\substack{n=1 \\ \text{when } m\neq n}}^{N} \mathrm{E}\{x(m)x(n)\}\{\frac{1}{2}[\ \cos(2\pi k\frac{(m\ +\ n)}{N}) + \cos(2\pi k\frac{(m\ -\ n)}{N})\ ]\}$$

$$+ \sum_{\substack{m=1 \\ \text{when } m=n}}^{N} \mathrm{E}\{x^2(m)\}\{\frac{1\ +\ \cos(4\pi k\frac{m}{N})}{2}\}$$

$$= 0.5\sum_{\substack{m=1 \\ \text{when } m\neq n}}^{N}(0)\ +\ 0.5\sum_{\substack{m=1 \\ \text{when } m=n}}^{N}(0.5)\ +\ 0.5\sum_{\substack{m=1 \\ \text{when } m=n}}^{N} 0.5\cos(4\pi k\frac{m}{N})$$

Using the same argument that cosine sums to zero in one period, when $k = 1, 2, 3...N-1$

$$= \frac{\mathrm{N}}{4}$$

The imaginary part can also be shown to have a variance of $\frac{\mathrm{N}}{4}$ in the similar manner. We know from the CLT (Central Limit Theorem) that the sum of large number of i.i.d. random variables each with finite mean and variance will approximately follow the normal distribution. Applying the CLT,

$$\Omega_R \sim \mathcal{N}(0, \frac{\mathrm{N}}{4})$$
$$\Omega_I \sim \mathcal{N}(0, \frac{\mathrm{N}}{4})$$

which means Ω as defined in (4.5) would follow a Rayleigh distribution with scale parameter σ. Assuming w to be a Rayleigh random variable, recalling the pdf (probability density function) of Rayleigh distribution:

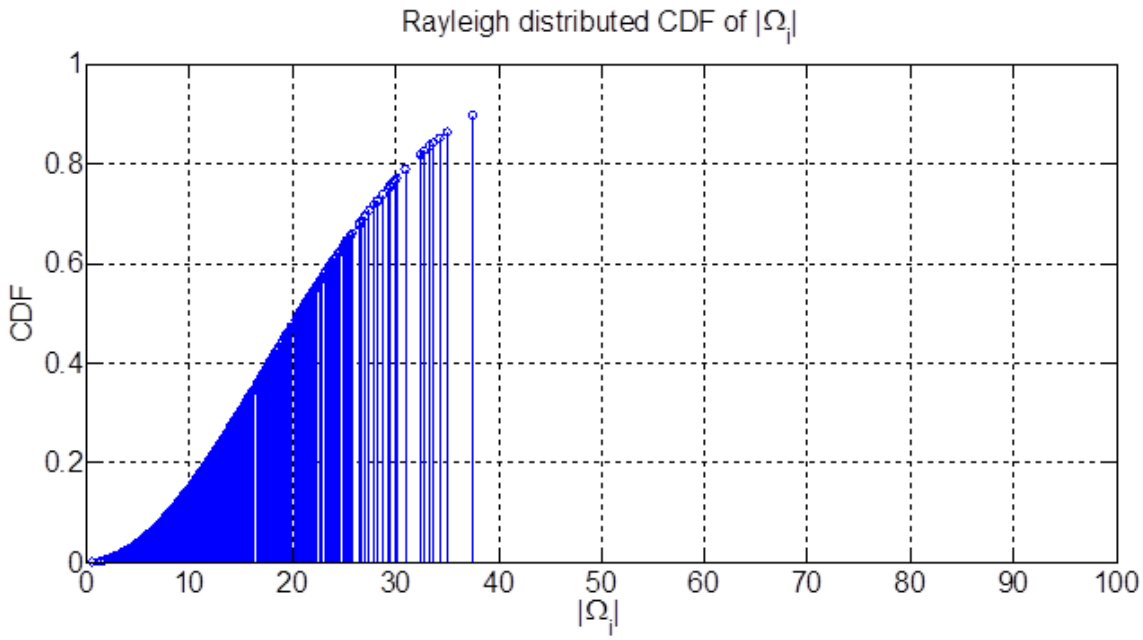

Figure 4.2. Cumulative distribution of magnitude spectrum of a random binary sequence with success probability of 0.5. The DC component has not been shown in the figure.

$$\begin{aligned} \mathrm{P}(w) &= \frac{w}{\sigma^2}\exp(-\frac{w^2}{2\sigma^2}) \quad \text{, for} \quad w \geq 0 \\ &= 0 \quad \text{, otherwise} \end{aligned}$$

where σ is the standard deviation of the Gaussian distribution.

Next, two different methods are employed to find the probability of obtaining good sequences for given values of τ and ρ.

As the Fourier coefficients are evaluated in the DFT from the same sequence, it needs to be checked if they are correlated. Let $|\Omega_i| = X$. Evaluating the covariance between different Fourier coefficients,

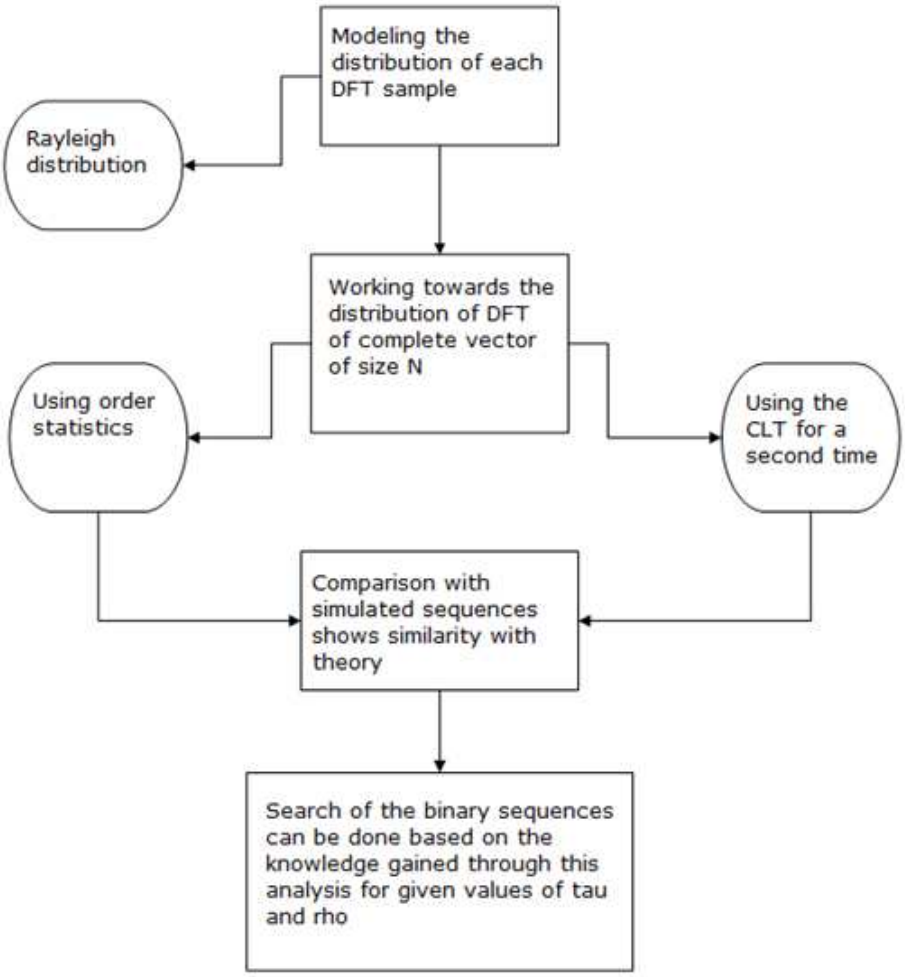

Figure 4.3. Steps in the analysis. Details for the parameters are same as in Figure 4.1.

$$\begin{aligned}\sigma_{X(k),X(l)} &= \mathrm{E}[\, X(k)X(l)\,] - \mathrm{E}[\, X(k)\,]\mathrm{E}[\, X(l)\,] \\ &= \mathrm{E}[\, (\sum_{m=1}^{N} x[m]\exp(-j2\pi k\frac{m}{N})\,)(\sum_{n=1}^{N} x[n]\exp(-j2\pi l\frac{n}{N})\,)\,] - 0, \\ &\quad \text{mean is zero as shown above} \\ &= \mathrm{E}[(\sum_{m=1}^{N} x[m]\cos(2\pi k\frac{m}{N}) - jx[m]\sin(2\pi k\frac{m}{N}))(\sum_{n=1}^{N} x[n]\cos(2\pi l\frac{n}{N}) - jx[n]\sin(2\pi l\frac{n}{N}))]\end{aligned}$$

Using trigonometric identities this can be simplified into,

$$= \mathrm{E}[\sum_{m=1}^{N}\sum_{n=1}^{N} x[m]x[n]\cos(2\pi\frac{(mk+nl)}{N}) - j\sum_{m=1}^{N}\sum_{n=1}^{N} x[m]x[n]\sin(2\pi\frac{(mk+nl)}{N})\ ]$$

$$= \mathrm{E}[\sum_{\substack{m=1 \\ \text{when } m=n}}^{N} x^2[m]\cos(2\pi\frac{(m(k+l))}{N}) + \sum_{\substack{m=1 \\ \text{when } m\neq n}}^{N}\sum_{n=1}^{N} x[m]x[n]\cos(2\pi\frac{(mk+nl)}{N})$$

$$- j\sum_{\substack{m=1 \\ \text{when } m=n}}^{N} x^2[m]\sin(2\pi\frac{(m(k+l))}{N}) - j\sum_{\substack{m=1 \\ \text{when } m\neq n}}^{N}\sum_{n=1}^{N} x[m]x[n]\sin(2\pi\frac{(mk+nl)}{N})]$$

After moving the expectation inside,

$$= [\sum_{\substack{m=1 \\ \text{when } m=n}}^{N} \mathrm{E}(x^2[m])\cos(2\pi\frac{(m(k+l))}{N}) + \sum_{\substack{m=1 \\ \text{when } m\neq n}}^{N}\sum_{n=1}^{N} \mathrm{E}(x[m]x[n])\cos(2\pi\frac{(mk+nl)}{N})$$

$$- j\sum_{\substack{m=1 \\ \text{when } m=n}}^{N} \mathrm{E}(x^2[m])\sin(2\pi\frac{(m(k+l))}{N}) - j\sum_{\substack{m=1 \\ \text{when } m\neq n}}^{N}\sum_{n=1}^{N} \mathrm{E}(x[m]x[n])\sin(2\pi\frac{(mk+nl)}{N})]$$

$$= [\sum_{\substack{m=1 \\ \text{when } m=n}}^{N} 0.5\cos(2\pi\frac{(m(k+l))}{N}) + \sum_{\substack{m=1 \\ \text{when } m\neq n}}^{N}\sum_{n=1}^{N} 0.25\cos(2\pi\frac{(mk+nl)}{N})$$

$$- j\sum_{\substack{m=1 \\ \text{when } m=n}}^{N} 0.5\sin(2\pi\frac{(m(k+l))}{N}) - j\sum_{\substack{m=1 \\ \text{when } m\neq n}}^{N}\sum_{n=1}^{N} 0.25\sin(2\pi\frac{(mk+nl)}{N})]$$

When $(\ m(k+l)\ ) < N$ and $(mk+nl) < N$ cosine and sine sum to zero over a period, hence

$$\sigma_{X(k),X(l)} = 0 \tag{4.6}$$

The correlation between the Fourier coefficients is found to be negligible even though they are obtained from the same binary sequence. Though we have not explicitly proven that their joint distribution is Gaussian, we assume them to be independent.

4.2.1 Using order statistics

Order statistics can be used to obtain the probability that a given binary sequence has at least ρ values in its DFT that are less than or equal to τ. As the presence of enough nulls in the frequency domain of random binary sequence is the most important characteristic needed for interference cancellation, this analysis helps us to get idea on the amount of search to be done. We know $|\Omega_i| = X$. Let N = 1000 and τ = 5. Then from the assumption of Rayleigh distribution,

$$\begin{aligned} P_\tau \equiv P(X \leq \tau) &= 1 - P(X > \tau) \\ &= 1 - \exp(\frac{-\tau^2}{2\sigma^2}) \\ &= 1 - 0.9048 \\ &= 0.0952 \end{aligned} \tag{4.7}$$

which can be taken as the success probability in order statistics. The order statistics can be applied if we arrange the values taken by the random variable X in ascending order. So we will have,

$$X_{(1)} < X_{(2)} < X_{(3)}..... < X_{(N)}$$

Applying order statistics, and substituting P_τ = 0.0952 and $\rho = 60$,

$$\begin{aligned} P_{\tau,\rho} &= P(\{\rho^{th} \text{ smallest of } X_{(1)}, X_{(2)}, X_{(3)}.....X_{(N/2)}\} \leq \tau) \\ &= \sum_{l=\rho}^{N/2} \binom{N/2}{l} P_\tau^l (1 - P_\tau)^{N/2-l} \\ &= \sum_{l=60}^{500} \binom{500}{l} (0.0952)^l (0.9048)^{500-l} \\ &= 0.038 \end{aligned}$$

Though this probability gives estimate of searching for 60 nulls, as the DFT of real sequences is symmetric in reality we obtain 120 nulls in an N-sized sequence. In general, this probability quantifies the search and tradeoff needed. For higher values of N, the order statistics approach will be computationally intensive and can also result in approximation errors. So, another approach is made using a second Gaussian approximation as given below.

4.2.2 Using Gaussian approximation

The CLT provides motivation to look for a better approach in the probability analysis of estimating the amount of search to be done to obtain sequences suited for the envisioned interference cancellation. As it has been stated, the random variable corresponding to the $|DFT|$ can be modeled using a Rayleigh distribution. We define a new random variable modeled as,

$$\begin{aligned} X_i = 1, \text{ if } \quad & |\Omega_i(k)| \leq \tau \text{ and} \\ = 0, & \text{ else} \end{aligned}$$

Essentially, this random variable follows a Bernoulli distribution with a success probability of P_τ which is the probability that a given bin in the DFT, $|\Omega_i(k)|$ is less than τ. Now using the random variable X, we find the probability of spectral nulls in the DFT $|\Omega_i(k)|$ for a given value of ρ by,

$$P(\quad (\sum_{i=1}^{N} X_i) \geq \rho \quad)$$

For a given value of ρ and τ, by bringing in the CLT here we can find the probability of obtaining corresponding sequences. Applying the CLT, we have

$$\frac{\sum_{i=1}^{N/2} X_i - \mathrm{E}[X_i]\frac{N}{2}}{\sqrt{\frac{N}{2}\mathrm{Var}[X_i]}} \quad \sim \quad \mathcal{N}(0,1) \tag{4.8}$$

where $E[X_i] = P_\tau$ and $Var[X_i] = P_\tau - P_\tau^2$

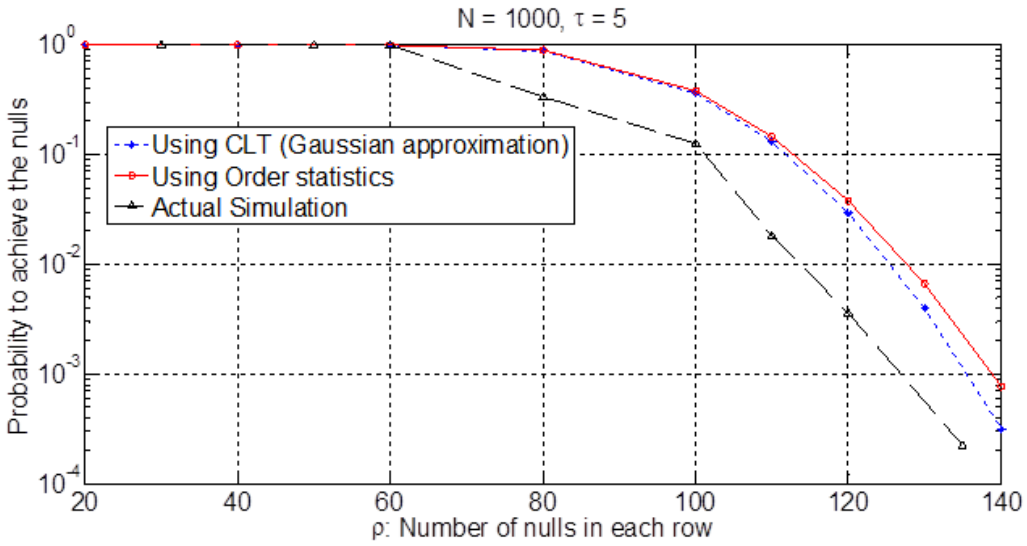

Figure 4.4. Comparison of the approximations with actual simulation (the reciprocal of number of search iterations in simulation was taken for comparison).

Taking the same example as in order statistics, with $\tau = 5$, $\rho = 60$, $N = 1000$ we will need to find $P(\ (\sum_{i=1}^{500} X_i) \geq 60\ )$,

With the assumption of independence, applying the CLT,

$$\frac{\sum_{i=1}^{500} X_i - \mathrm{E}[X_i]500}{\sqrt{500\mathrm{Var}[X_i]}} \sim \mathcal{N}(0,1)$$

As evaluated above, P_τ = 0.0952. So, the mean is $E[X_i] = 0.0952$ (From (4.7) and (4.8)). Let the left hand side of the above be denoted by Y,

$$Y \sim \mathcal{N}(0,1)$$

Consider $P(\ \sum_{i=1}^{N/2} X_i \geq 60\ )$ which when simplified further becomes,

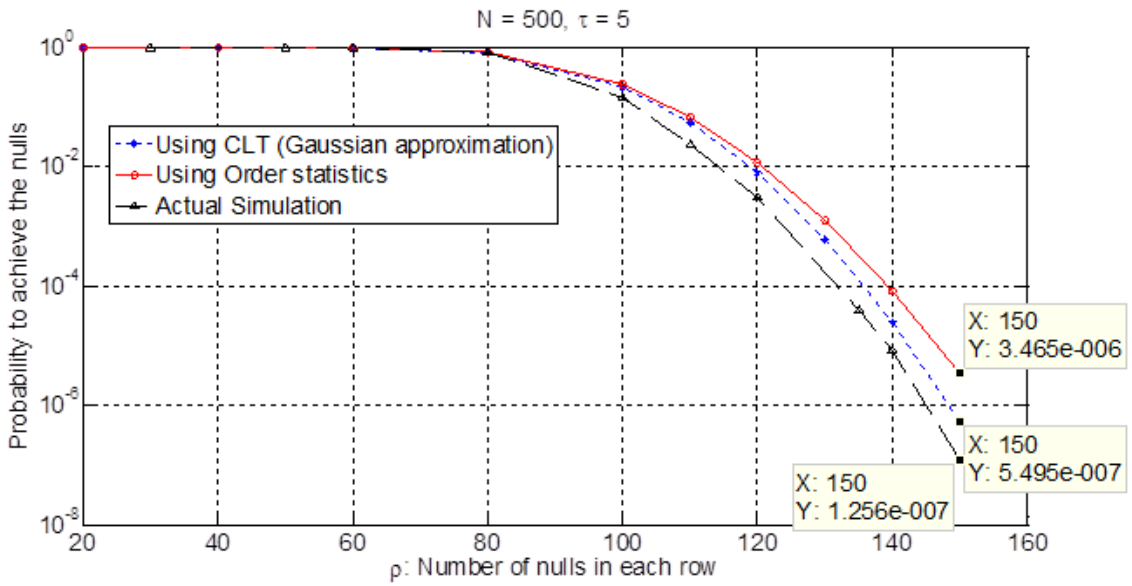

Figure 4.5. Comparison of the approximations with actual simulation (the reciprocal of number of search iterations in simulation was taken for comparison) for lower N

$$
\begin{aligned}
P_{\tau,\rho} \equiv P(\sum_{i=1}^{500} X_i \geq 60) &= P(\frac{\sum_{i=1}^{500} X_i - 0.0952 * 500}{\sqrt{500 * (0.0952 - 0.0952^2)}} \geq \frac{60 - 500 * 0.0952}{\sqrt{500 * (0.0952 - 0.0952^2)}}) \\
&= P(Y \geq \frac{12.41}{\sqrt{(500 * 0.0861)}}) \\
&= P(Y \geq 1.8927) \\
&= Q(1.8927) \text{ , where Q(x) is the Q-function} \\
&= 0.0292
\end{aligned}
$$

It is found that the probability estimated from the above two methods of order statistics and Gaussian approximation seems to be close to that of simulated sequences as shown in the Figure 4.4 where actual simulated numbers can also be seen. Though there is noticeable difference between the simulation and theory, the reason may not be attributed to the CLT as we can see that for $N = 500$ in the Figure 4.5, they appear much closer. As analytical and simulated values of P_τ are found to be very close, this difference may be attributed to the assumption of independence in the previous section.

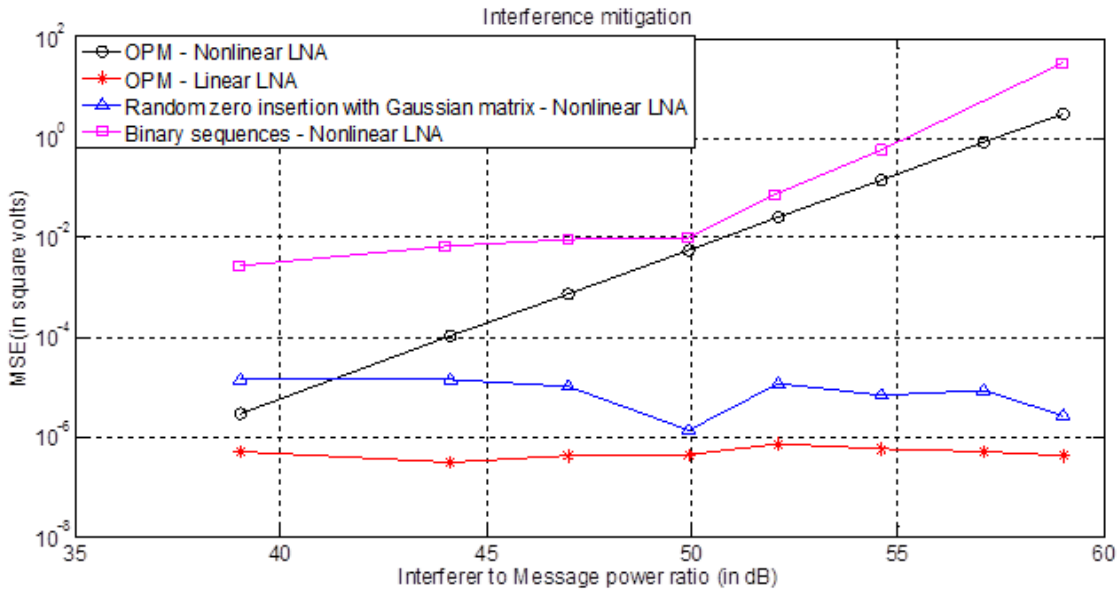

Figure 4.6. Comparison of MSE with OPM under different scenarios of interference power. The parameters used for binary sequences are (1) success probability for the binary sequence is 0.5 (2) $\tau = 4$, $N = 1000$, $s = 5$ (sparsity), ρ = 100 (3) The average signal energy in the sequences is about 500. Details for the figure for OPM and Gaussian matrix method are same as in the Figure 3.6

4.3 Usage of the sequences in wideband system

After obtaining the optimum random binary sequences we can use them to produce the switching pattern in the branches of the receiver shown in Figure 1.1. Assuming the selection of interference-free branches is possible, we discard the interference-affected branches and using the measurement matrix obtained from the resulting branches, we perform CS-based reconstruction in the following DSP.

Here we do not assume any specific knowledge of how to pick τ and ρ except from the information obtained from the calculation of $P_{\tau,\rho}$ for different values of τ and ρ. The analysis can provide only knowledge of how much computational effort is needed for the search and hence is not a direct indicator of selecting good pairs of (ρ, τ).

An example is provided to see how this analysis can be applied in practice. As seen the Figure 4.2, the probability of obtaining a null is in the leftmost part of the tail of the distri-

bution. The value of τ is picked by taking this into account. Upon estimating probability for different values of ρ, a value is chosen for ρ that has high probability. Using this pair (ρ, τ), binary sequences are created with the search algorithm flowchart of which is shown in the Figure 4.1.

The use of binary sequences in the presence of nonlinear LNA seems to perform worse compared to OPM in the same scenario as seen in Figure 4.6. As the LNA is driven more into nonlinear region, interference mitigation cannot be accomplished by using the near-nulls in the binary sequences as the nonlinearities become prominent. This can be attributed to the use of real binary sequences without any random insertion of spectral nulls verses idealized hardware assumption for the performance seen in the Figure 3.6.

CHAPTER 5

CONCLUSION

In this thesis, we have looked at the nonideal aspects of the RF front-end of wideband receivers which might become impeding blocks to interference cancellation schemes concentrated on compressed sensing techniques. Specifically we looked at how an interference mitigation scheme in the compressive domain fares in a realistic environment in the presence of nonlinear LNA and finite bit ADCs. Through simulations, it was found that interference mitigation cannot be performed at the DSP, due to the fact that the nonidealities present will result in irresolvable intermodulation components and corrupt the signal reconstruction. This has lead to the question of whether cancelling out the interferer before reaching the LNA is possible. It turned out that a matrix with randomly placed zeros in the frequency domain would serve this purpose well. Using this idea, encouraging results under very idealized hardware assumptions were obtained by performing CS measurements before the LNA.

Though this is theoretically promising, due to its real-world implementation complexity, hardware-friendly options are needed. Binary sequences offer a viable alternative to those of Gaussian measurement matrices in terms of practical hardware implementation and also have ability to form good CS measurement matrices. The switches that these sequences are obtained from are assumed to be ideal in nature in this thesis. It is observed that finding binary sequences which have many nulls in their frequency domain is nontrivial and requires careful selection of search parameters to avoid significant wasted effort. Theoretically, the probability of finding sequences with a given number of spectral nulls has been modeled and shown to be close to the actual search iterations in simulation.

Though binary sequences have advantage in terms of simplistic hardware implementation, it turns out that exhaustive search is needed to find sequences with a lot of near-nulls in the frequency domain which becomes more challenging when nonlinear LNA also needs to be taken into account. From the simulation of Figure 4.6, it can be said that interference cancellation using spectral nulls with binary sequences does not perform better than OPM for a nonlinear RF front-end.

5.1 Future work

Analysis of the selection of the proper ordered pairs (τ, ρ) for a given search complexity is a key future step. Nonlinear switches and nonlinearity in the LNA also influence this selection.

From CS results, it is known that $\{-1, +1\}$ matrices follow the RIP, while $\{0, 1\}$ matrices need a substantially higher number of rows to follow the RIP. The usage of Bernoulli matrices with elements $\{-1, +1\}$ instead of $\{0, 1\}$ can be explored for reduction in the total number of measurements, at a cost of increased complexity in implementation.

BIBLIOGRAPHY

[1] E. Candes, J. Romberg, and T. Tao, "Robust uncertainty principles: Exact signal reconstruction from highly incomplete frequency information", *IEEE Transactions on Information Theory*, Vol. 52: pp. 489-509, Februrary 2006.

[2] E. J. Candès and J. Romberg. "Sparsity and incoherence in compressive sampling", *Inverse Problems*, 23 969-985.

[3] R. Baraniuk, M. Davenport, R. DeVore, and M. Wakin, "A simple proof of the restricted isometry property for random matrices," *Constructive Approximation 28 (2008)* , no. 3, pp. 253-263.

[4] E. J. Candès, "Compressive sampling," *Proceedings of the International Congress of Mathematicians* , Madrid, Spain, 2006.

[5] Wei Wang, M. J. Wainwright , K. Ramchandran, "Information-Theoretic Limits on Sparse Signal Recovery: Dense versus Sparse Measurement Matrices" , in *IEEE Transactions on Information Theory* , Vol. 56 :pp 2967-2979, June 2010.

[6] Mark A. Davenport, Marco F. Duarte, Yonina C. Eldar and Gitta Kutyniok, "Introduction to Compressed Sensing," in *Compressed Sensing: Theory and Applications*, Y. Eldar and G. Kutyniok, eds., Cambridge University Press, 2011

[7] E. J. Candès and M. Wakin, "An introduction to compressive sampling," *IEEE Signal Processing Magazine* , March 2008 21-30.

[8] E. Arias-Castro and Y. C. Eldar, "Noise folding in compressed sensing," *IEEE Signal Processing Letters*, Vol.18, No.8, August 2011.

[9] M. A. El-Tanani and G. M. Rebeiz "High-Performance 1.5-2.5GHz RF-MEMS Tunable Filters for Wireless Applications," *IEEE Transactions on Microwave Theory and Techniques*, Vol. 58: pp. 1629-1637, June 2010.

[10] E. A. Keehr and A. Hajimiri, "Successive Regeneration and Adaptive Cancellation of Higher Order Intermodulation Products in RF Receivers," *IEEE Transactions on Microwave Theory and Techniques*, Vol. 59: pp. 1379-1396, May 2011.

[11] Jason N. Laska, Sami Kirolos, Marco F. Duarte, Tamer S. Ragheb, Richard G. Baraniuk,Yehia Massoud, "Theory and Implementation of an Analog-to-Information Converter using Random Demodulation", in *Proc. 2007 IEEE Int. Symp. Circuits and Systems (ISCAS)* , New Orleans, LA, May 2007, pp.1959–1962.

[12] M. Wakin, J. Laska, M. Duarte, D. Baron, S. Sarvotham, D. Takhar, K. Kelly, and R. Baraniuk, "An architecture for compressive imaging", *Proc. Intl. Conf. Image Proc.* (Atlanta), 2006.

[13] J. N. Laska, S. Kirolos, Y. Massoud, R. G. Baraniuk, A. C. Gilbert, M. Iwen, and M. J. Strauss, "Random sampling for analog-to-information conversion of wideband signals", *IEEE Dallas/CAS Workshop on Design, Applications, Integration and Software*, Oct. 2006.

[14] J. Tropp, M. Wakin, M. Duarte, D. Baron, and R. Baraniuk, "Random filters for compressive sampling and reconstruction", in *Proc. IEEE Int. Conf. Acoust., Speech, and Signal Processing (ICASSP)* , Toulouse, France, May 2006.

[15] M. Davenport, P. Boufounos, and R. Baraniuk, "Compressive Domain Interference Cancellation", in *Proc. Work. Struc. Parc. Rep. Adap. Signaux (SPARS)*, Saint-Malo, France, Apr. 2009.

[16] S. Hwang, S. Jang, D. Kim, and J. Seo,"An MMSE-based compressive domain interference cancellator for wideband systems", *International Conference on Computer and Automation Engineering* , Feb. 2010.

[17] M. A. Davenport, S. R. Schnelle, J. P. Slavinsky, R. G. Baraniuk, M. B. Wakin, and P. T. Boufounos, "A Wideband Compressive Radio Receiver", in *Military Communications Conference (MILCOM), San Jose, California*, Oct. 2010.

[18] Dennis L. Goeckel, Robert W. Jackson, Marco F. Duarte, Proposal submitted to NSF, Oct 2011.

[19] R. H.Walden,"Analog-to-digital converter survey and analysis," *IEEE Journal.Selected Areas in Communications*, vol. 17, no. 4, pp. 539–550, Apr. 1999

[20] B. Razavi, *RF Microelectronics*. Prentice Hall, 1998

[21] Stephen R. Becker, *Practical Compressed Sensing: modern data acquisition and signal processing*, Phd Thesis, 2011

[22] V. Chandar, *A negative result concerning explicit matrices with the restricted isometry property*

[23] *Texas Instruments online tutorial on WiFi Adjacent Channel Interference and Wikipedia resources*